HPLC-ICP-AES technique for the screening of $[XW_{11}NbO_{40}]^{n-}$ aqueous solutions

Alexandra A. Shmakova[a,b], Maria M. Akhmetova[a,b], Victoria V. Volchek[a,b], Tamara E. Romanova[a,b], Ilya Korolkov[a,b], Dmiri G. Sheven'[a], Sergey A. Adonin*[a,b], Pavel A. Abramov*[a,b], Maxim N. Sokolov[a,b]

Supporting information

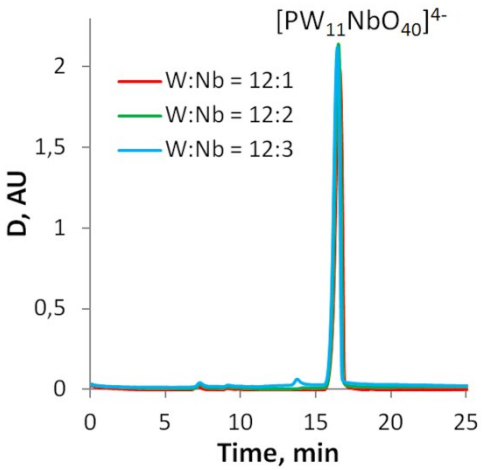

Fig. S1. The HPLC-UV chromatograms of reaction product for different initial W:Nb ratios. The separation conditions: ProntoSIL 120-5-C18AQ, eluents: A – 0.04% TBAH, 1% AcOH (pH 2.7), B – acetonitrile; gradient mode: 0–4.6 min, 0–30% B; 4.6–14.2 min, 30-55% B; 14.2–23.1 min, 55% B; 23.1–29.2 min, 100% B; flow rate – 0.13 mL min^{-1}.

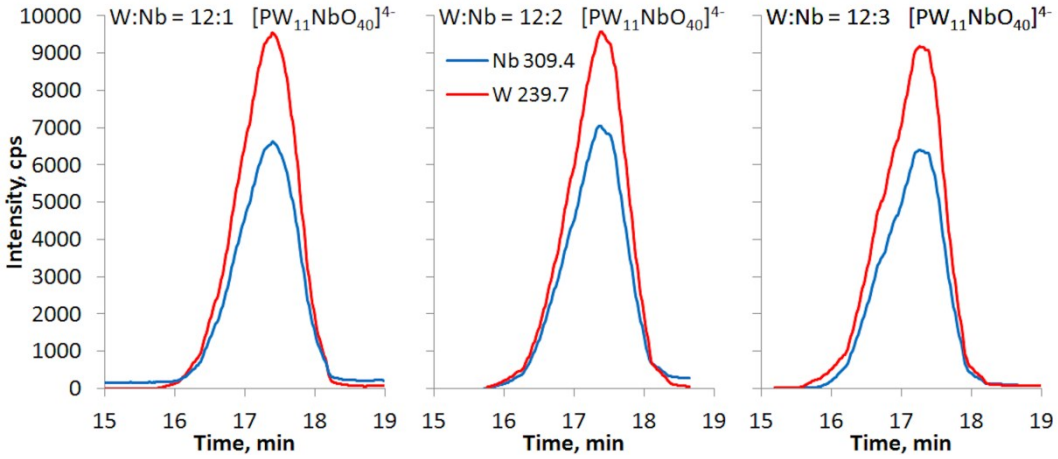

Fig. S2. The HPLC-ICP-AES chromatograms of reaction product at different initial W:Nb ratios in coordinates "retention time–line intensity". Separation conditions: the same as in Fig. S1.

Table S1. Atomic ratios W/Nb for $[PW_{11}NbO_{40}]^{4-}$ peak calculated from HPLC-ICP-AES-data.

W / Nb	Nb 202.9 nm	Nb 309.4 nm	Nb 316.3	Nb 319.4
W 202.6 nm	11.6±0.7	11.2±0.6	10.6±0.6	10.9±0.7
W 209.8 nm	11.4±0.6	11.1±0.5	10.7±0.5	10.8±0.5
W 229.4 nm	11.5±0.6	11.4±0.6	10.9±0.5	10.7±0.6
W 239.7 nm	11.1±0.6	10.9±0.5	10.8±0.5	10.7±0.5

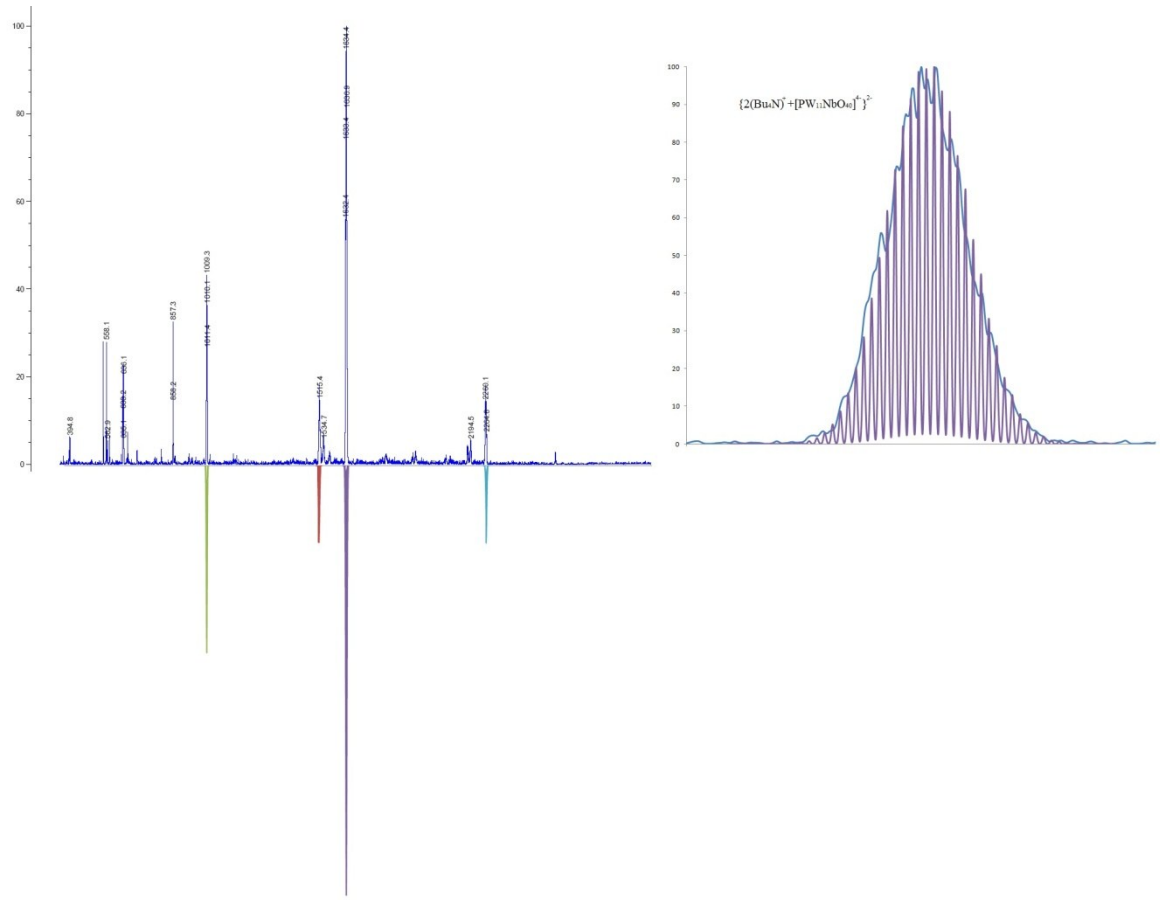

Fig. S3. ESI-MS spectrum of $[PW_{11}NbO_{40}]^{4-}$ after the reaction of $(TBA)_4H_3[PW_{11}O_{39}]$ and Nb-Ox for 12 hours at 60°C in DMF.

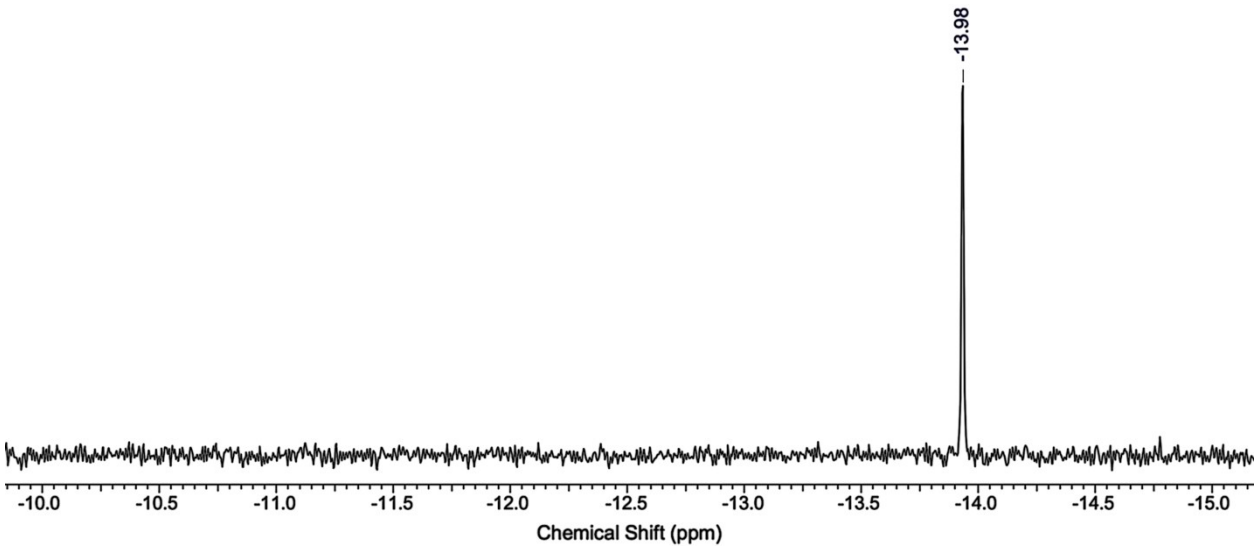

Fig. S4. ^{31}P NMR spectrum of $(TBA)_4[PW_{11}NbO_{40}]$ in CD_3CN.

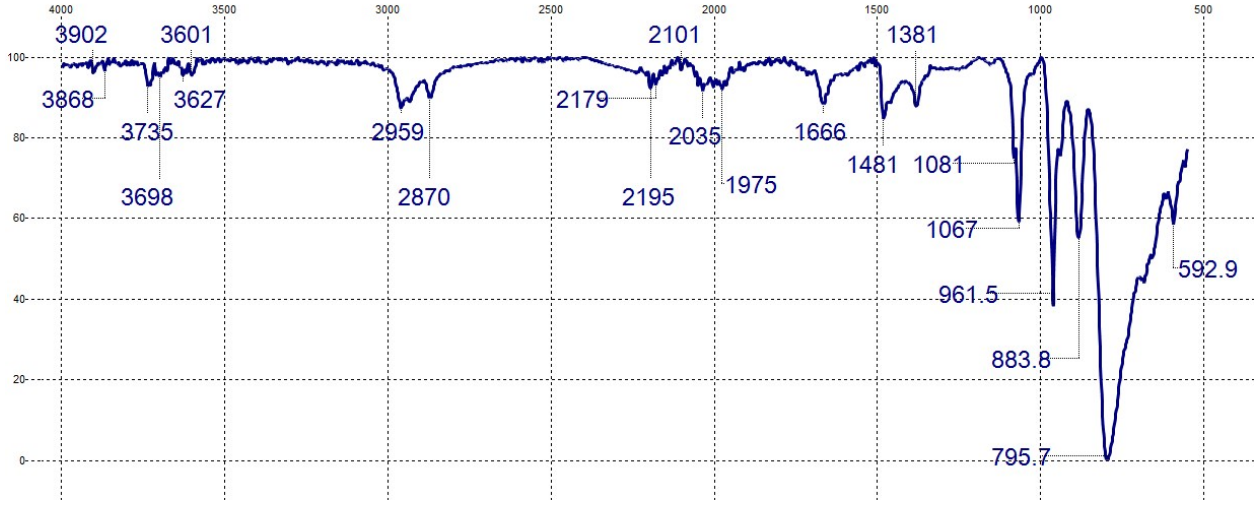

Fig. S5. FT-IR of $(TBA)_4[PW_{11}NbO_{40}]$.

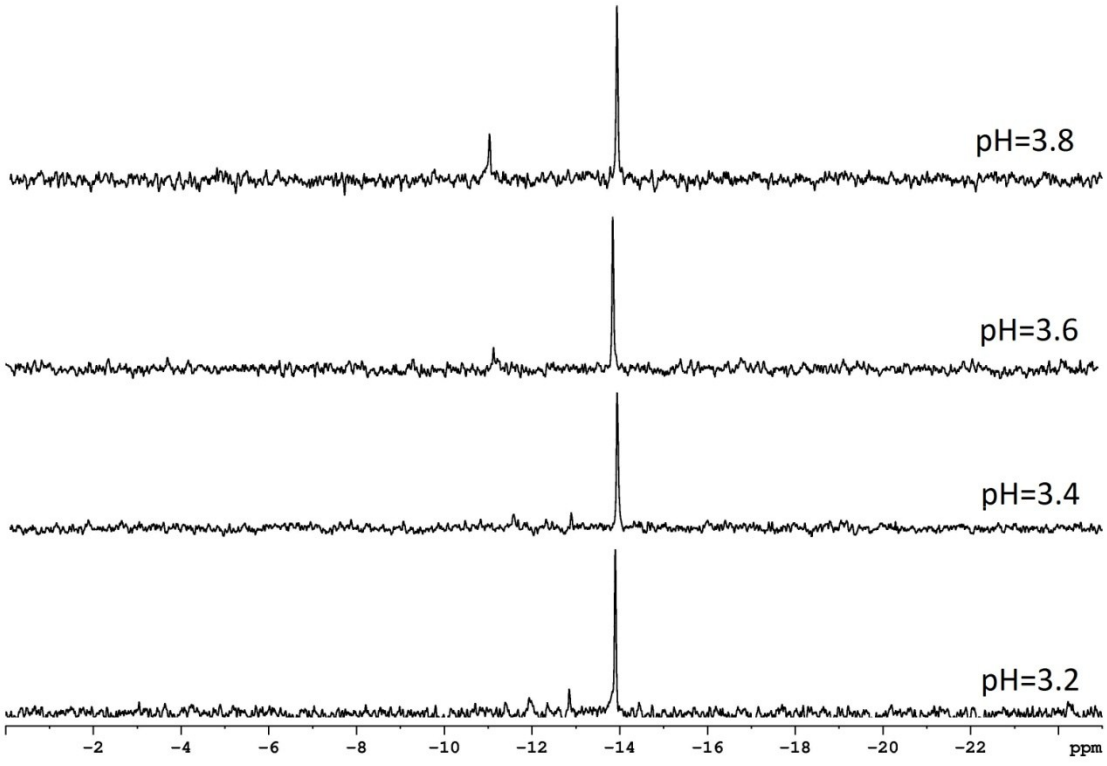

Fig. S6. pH dependency of ^{31}P NMR chemical shifts for $[PW_{11}NbO_{40}]^{4-}$ between pH 3.2 and 3.8.

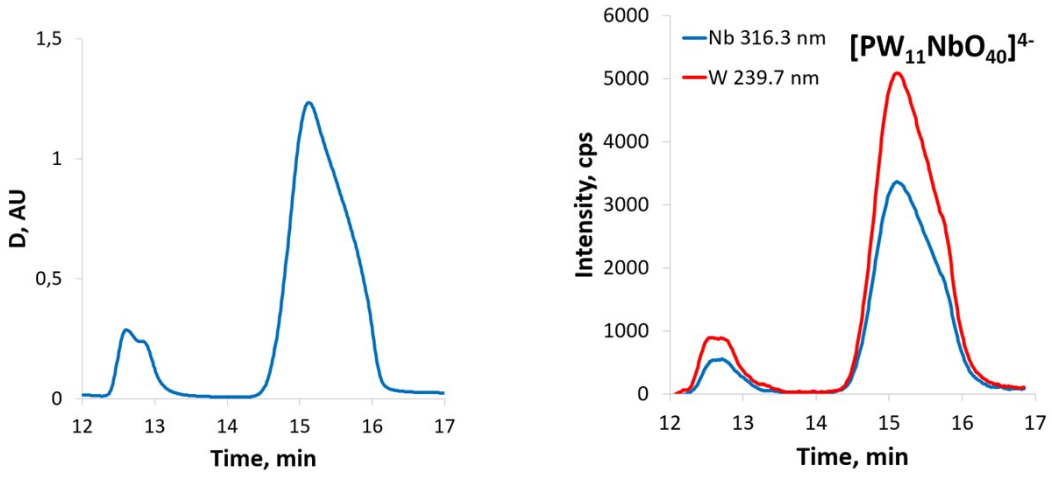

Fig. S7. a) The HPLC-UV chromatogram (left) and HPLC-ICP-AES chromatogram (right) of aged $[PW_{11}NbO_{40}]^{4-}$ solution at pH = 3.15.

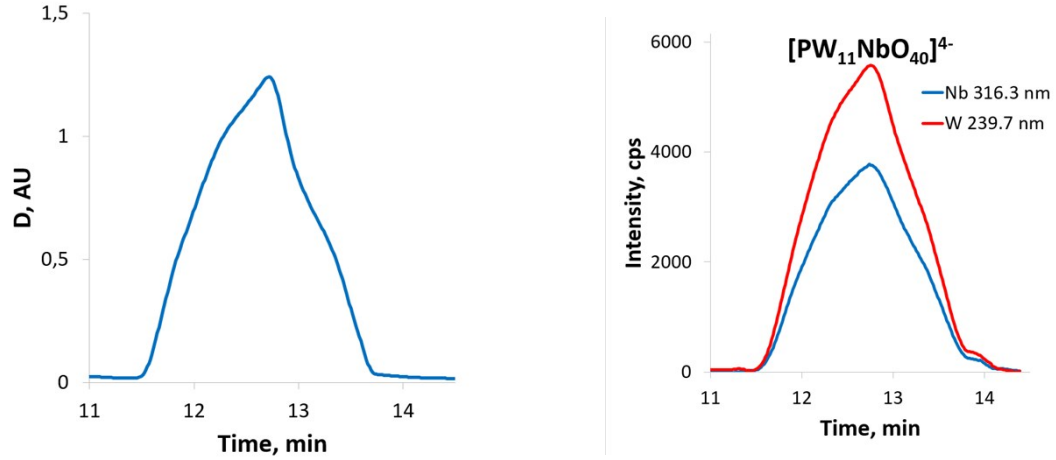

Fig. S7. b) The HPLC-UV chromatogram (left) and HPLC-ICP-AES chromatogram (right) of aged $[PW_{11}NbO_{40}]^{4-}$ solution at pH = 4.0.

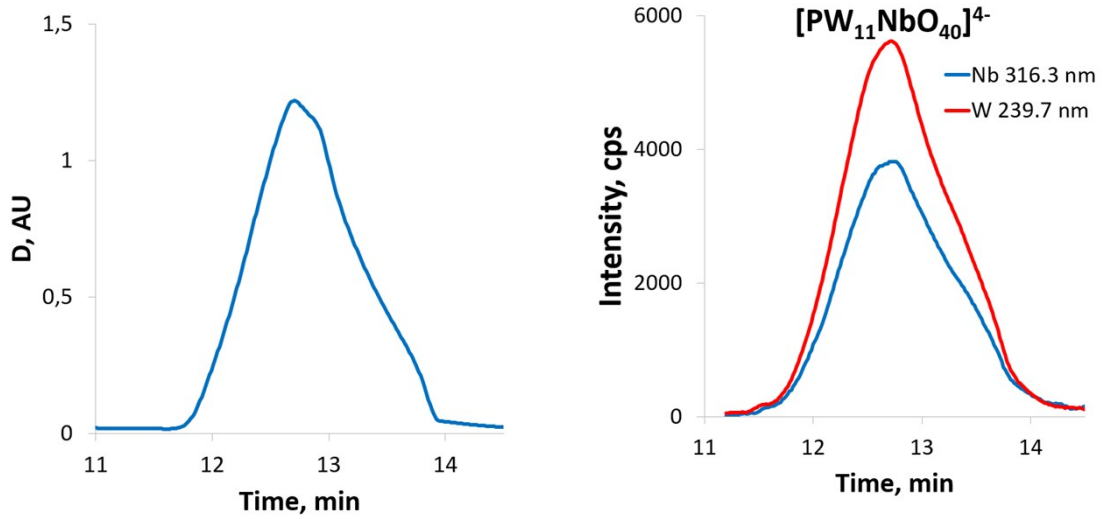

Fig. S7. c) The HPLC-UV chromatogram (left) and HPLC-ICP-AES chromatogram (right) of aged $[PW_{11}NbO_{40}]^{4-}$ solution at pH = 4.6.

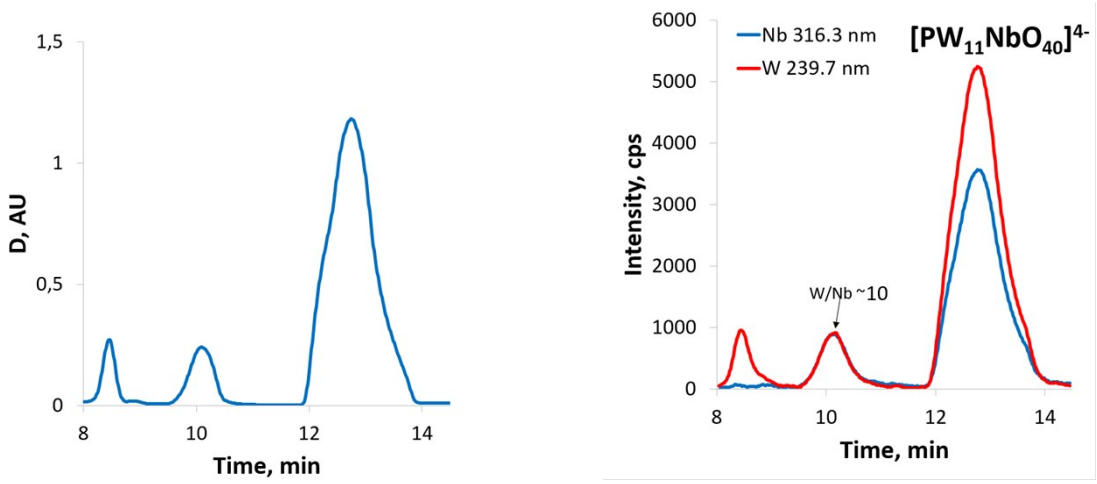

Fig. S7. d) The HPLC-UV chromatogram (left) and HPLC-ICP-AES chromatogram (right) of aged $[PW_{11}NbO_{40}]^{4-}$ solution at pH = 5.5.

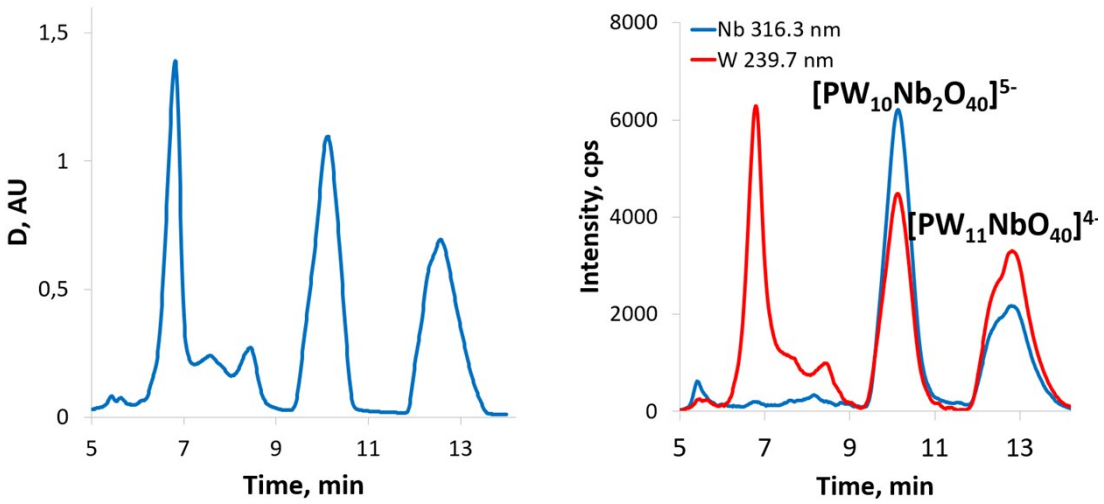

Fig. S7. e) The HPLC-UV chromatogram (left) and HPLC-ICP-AES chromatogram (right) of aged $[PW_{11}NbO_{40}]^{4-}$ solution at pH = 6.0.

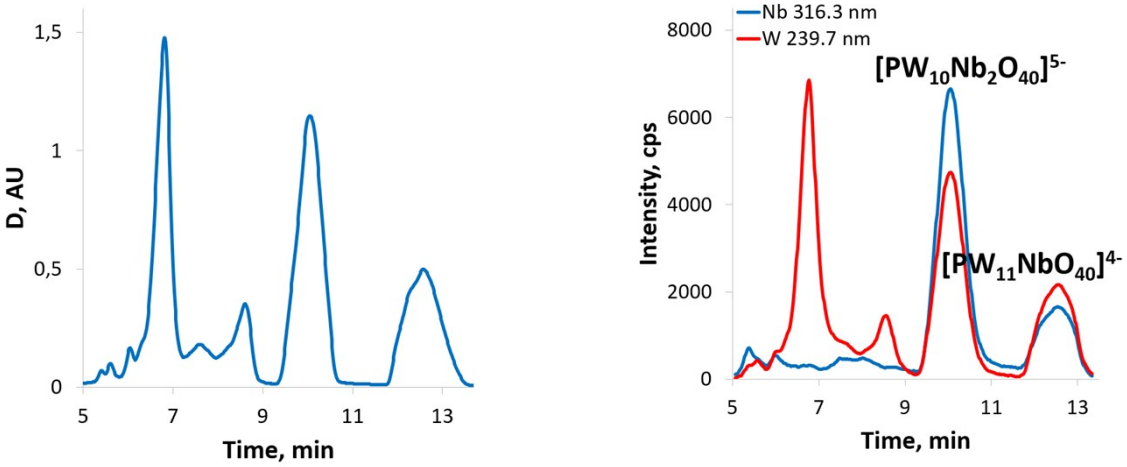

Fig. S7. f) The HPLC-UV chromatogram (left) and HPLC-ICP-AES chromatogram (right) of aged $[PW_{11}NbO_{40}]^{4-}$ solution at pH = 6.4.

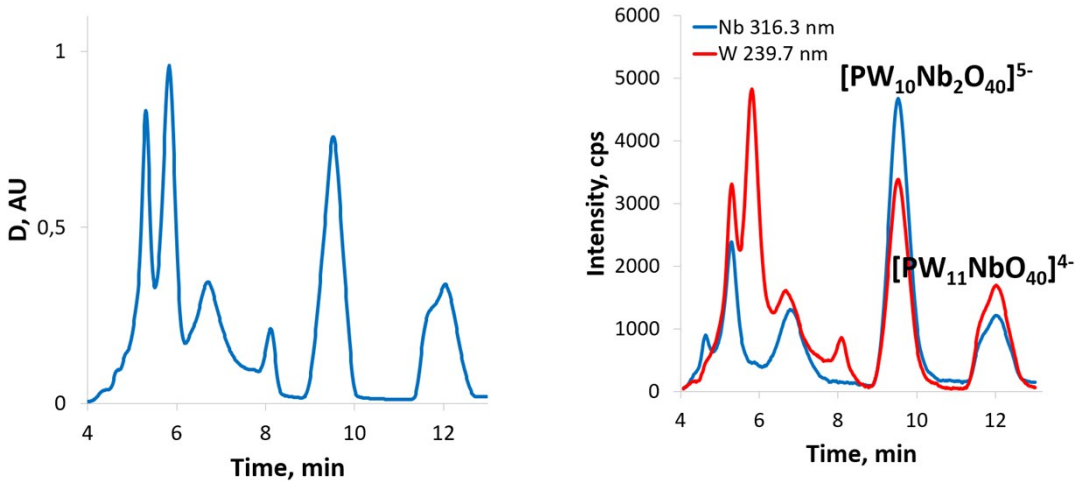

Fig. S7. g) The HPLC-UV chromatogram (left) and HPLC-ICP-AES chromatogram (right) of aged $[PW_{11}NbO_{40}]^{4-}$ solution at pH = 7.08.

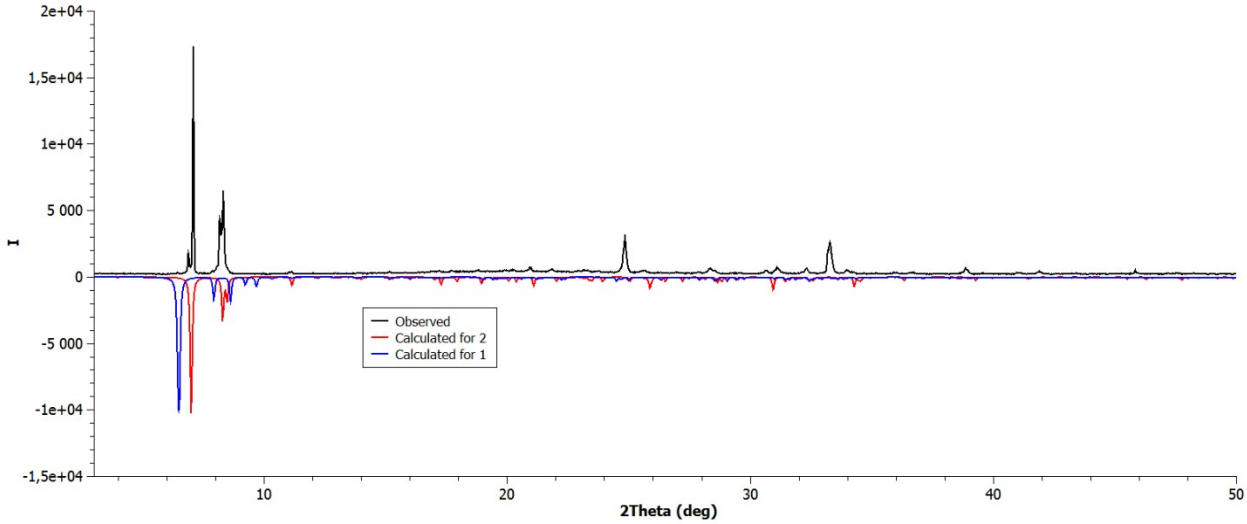

Fig. S8. XRPD patterns for **2** in vaseline oil.

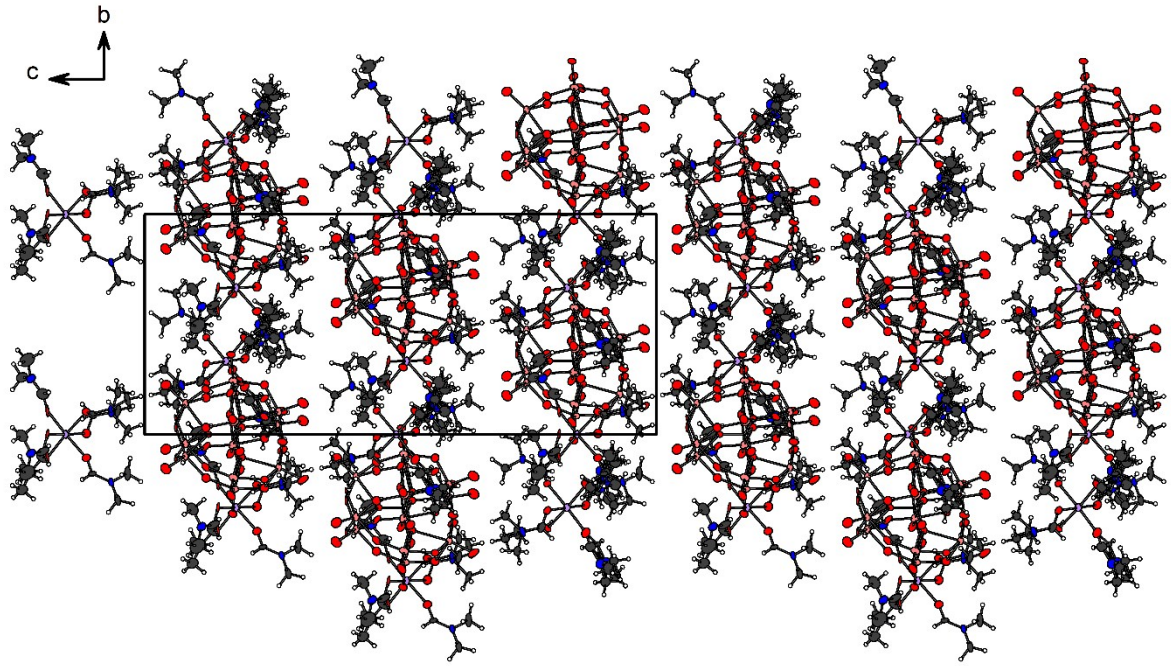

Fig. S9. Crystal packing of **2**.

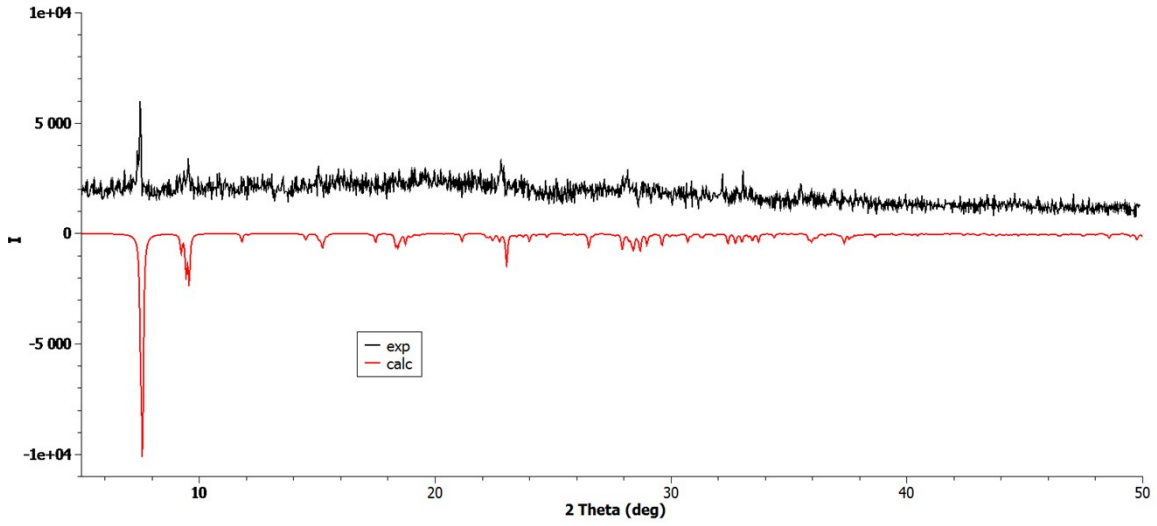

Fig. S10. XRPD pattern for **3** in vaseline oil.

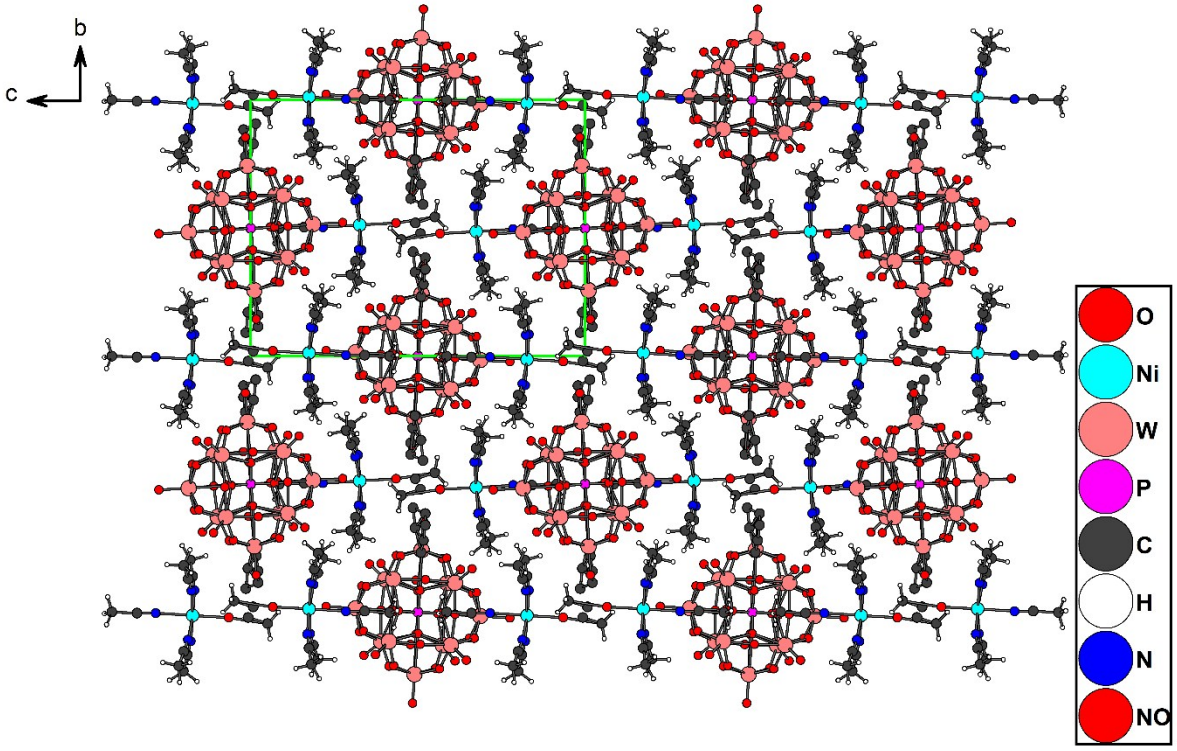

Fig. S11. Crystal packing of **3**.

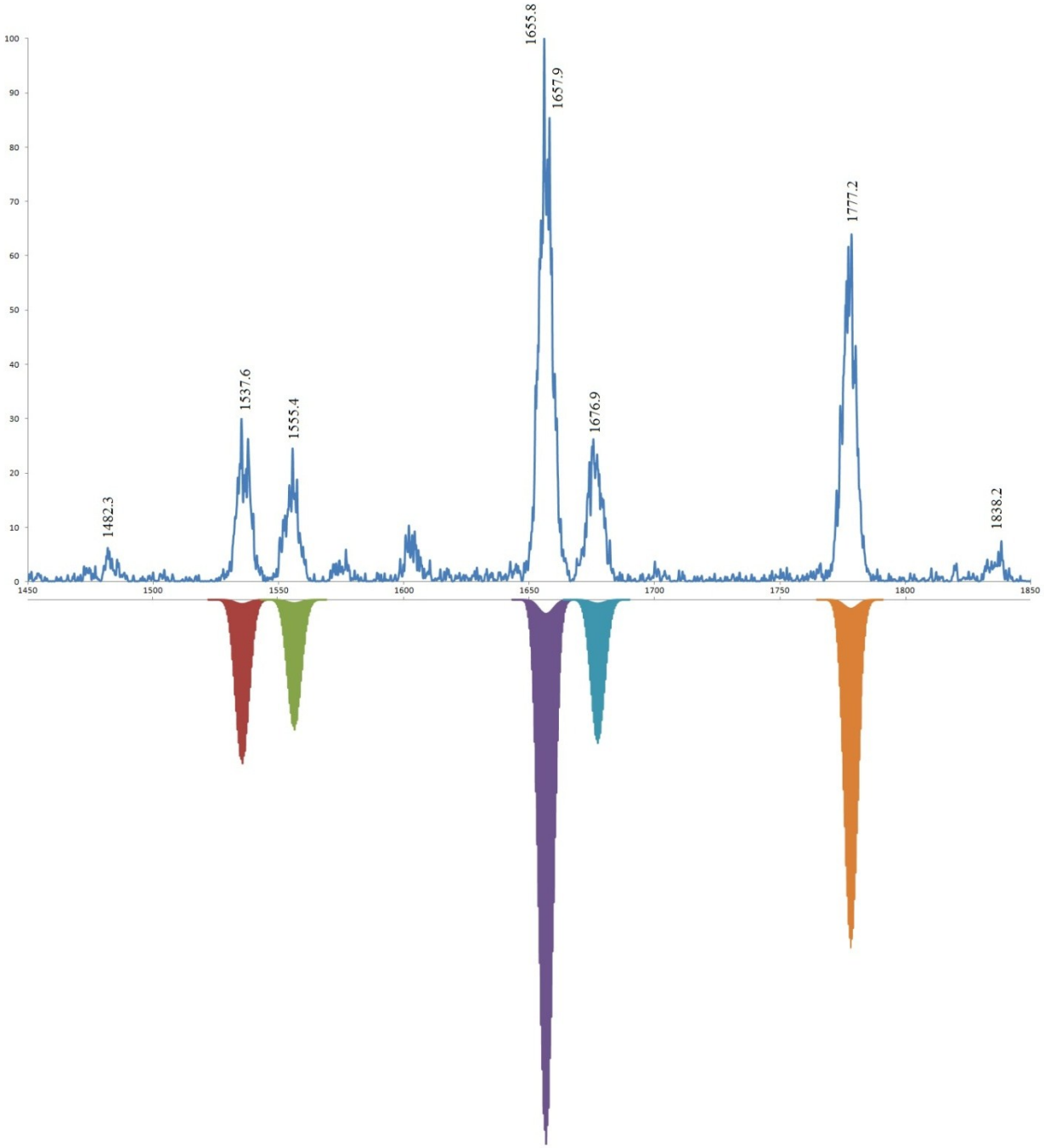

Fig. S12. ESI-MS(-) spectrum of **5** in acetonitrile, up - experimental, down - calculated.

Table S2. Peak assignment for ESI-MS(-) spectrum of **5** in acetonitrile.

Mass/charge	Assignment
1537,6	$\{(Bu_4N)^+ + 2H^+ + [GeW_{11}NbO_{40}]^{5-}\}^{2-}$
1555,4	$\{(Bu_4N)^+ + 2H^+ + [GeW_{11}NbO_{40}]^{5-} + MeCN\}^{2-}$
1655,8	$\{2(Bu_4N)^+ + H^+ + [GeW_{11}NbO_{40}]^{5-}\}^{2-}$
1676,9	$\{2(Bu_4N)^+ + H^+ + [GeW_{11}NbO_{40}]^{5-} + MeCN\}^{2-}$
1777,2	$\{3(Bu_4N)^+ + [GeW_{11}NbO_{40}]^{5-}\}^{2-}$

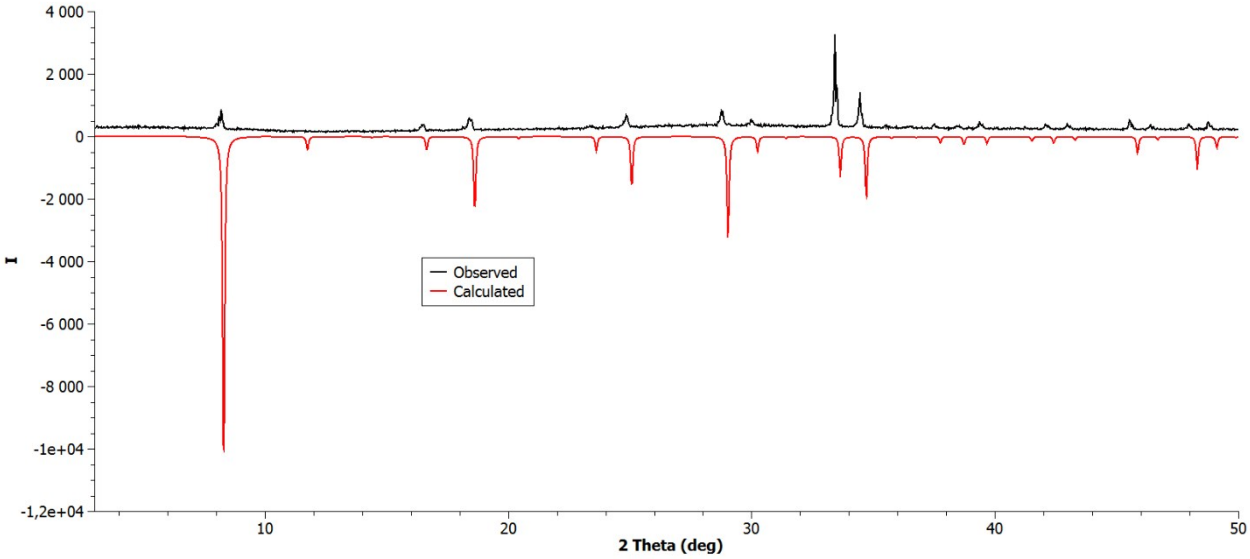

Fig. S13. XRPD pattern for **4**.

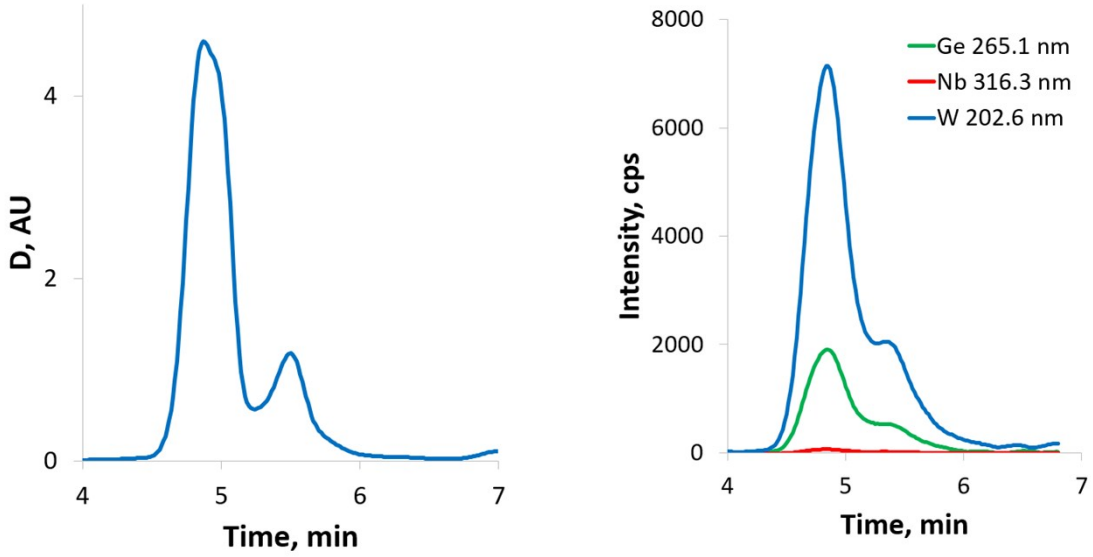

Fig. S14. The HPLC-UV chromatogram (left) and HPLC-ICP-AES chromatogram (right) of $[GeW_{11}O_{39}]^{8-}$ solution.

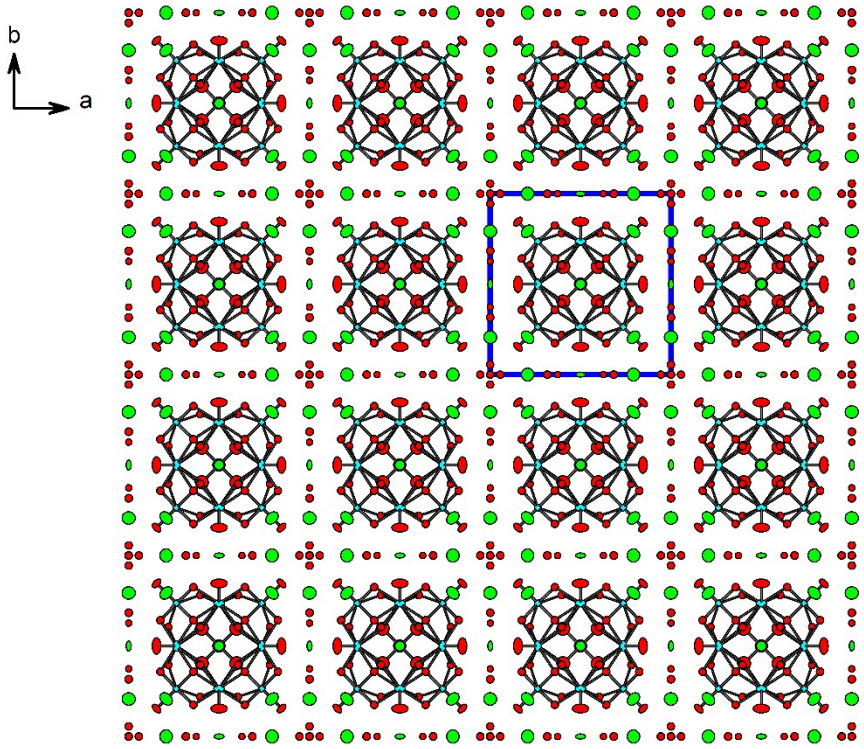

Fig. S15. Crystal packing of **4**.

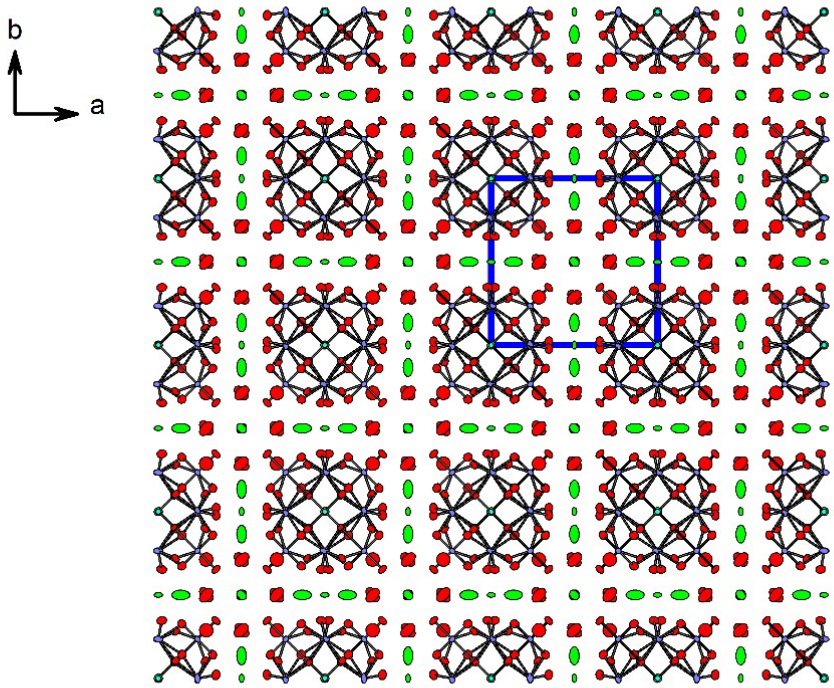

Fig. S16. Crystal packing of $K_8[GeW_{11}O_{39}]\cdot 13H_2O$.

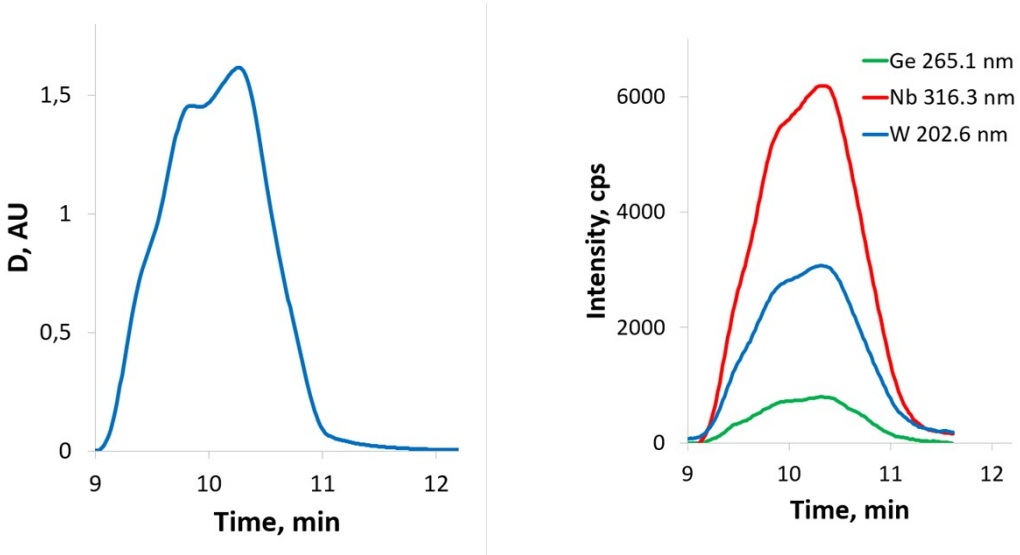

Fig. S17. The HPLC-UV chromatogram (left) and HPLC-ICP-AES chromatogram (right) of $[GeW_{11}NbO_{39}]^{5-}$ solution.

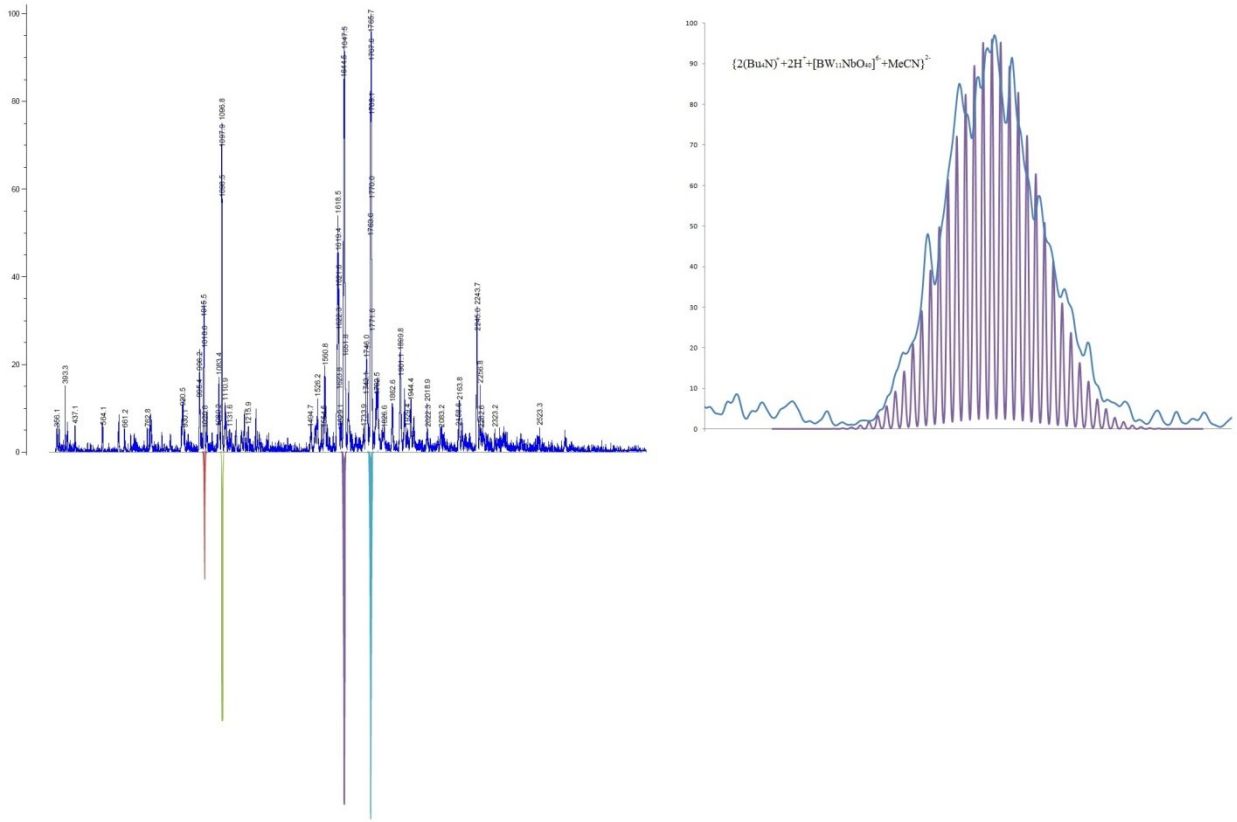

Fig. S18. ESI-MS(-) spectrum of **6** in acetonitrile.

Table S3. Peak assignment for ESI-MS(-) spectrum of **6** in acetonitrile.

Mass/charge	Assignment
1015,5	$\{(Bu_4N)^+ + 2H^+ + [BW_{11}NbO_{40}]^{6-} + MeCN\}^{3-}$
1096,8	$\{2(Bu_4N)^+ + H^+ + [BW_{11}NbO_{40}]^{6-} + MeCN\}^{3-}$
1647,5	$\{(Bu_4N)^+ + 3H^+ + [BW_{11}NbO_{40}]^{6-} + MeCN\}^{2-}$
1765,7	$\{2(Bu_4N)^+ + 2H^+ + [BW_{11}NbO_{40}]^{6-} + MeCN\}^{2-}$

Table S4. Experimental details.

Parameter	**2**	**3**	**4**
Chemical formula	$C_{36}H_{84}Co_2N_{12}O_{52}PW_{12}$	$C_{27}H_{33}N_{11}Ni_2O_{41}PW_{12}$	$GeK_5O_{50.29}W_{12}$
M_r	3872.18	3522.23	3278.95
Crystal system, space group	Trigonal, *R*3	Monoclinic, $P2_1/n$	Cubic, $Pm\bar{3}m$
Temperature (K)	130	130	296
a, *b*, *c* (Å)	15.8751 (6), 15.8751 (6), 31.9698 (14)	12.6148 (8), 14.6506 (7), 19.8436 (12)	10.6496 (1), 10.6496 (1), 10.6496 (1)
α, β, γ (°)	90, 90, 120	90, 105.190 (6), 90	90, 90, 90
V (Å^3)	6977.6 (6)	3539.3 (4)	1207.81 (3)
Z	3	2	1
μ (mm^{-1})	15.22	20.04	29.60
Crystal size (mm)	0.22 × 0.22 × 0.06	0.15 × 0.10 × 0.08	0.10 × 0.10 × 0.10
Diffractometer	New Xcalibur, AtlasS2	New Xcalibur, AtlasS2	Bruker Apex Duo
Absorption correction	Multi-scan *CrysAlis PRO* 1.171.38.41 (Rigaku Oxford Diffraction, 2015) Empirical absorption correction using spherical harmonics, implemented in SCALE3 ABSPACK scaling algorithm.	Multi-scan *CrysAlis PRO* 1.171.38.41 (Rigaku Oxford Diffraction, 2015) Empirical absorption correction using spherical harmonics, implemented in SCALE3 ABSPACK scaling algorithm.	Multi-scan *SADABS* (Bruker-AXS, 2004)
T_{min}, T_{max}	0.144, 1.000	0.321, 1.000	0.551, 0.747
No. of measured, independent and observed [$I > 2\sigma(I)$] reflections	6745, 4974, 4549	27962, 6230, 3763	6866, 507, 443
R_{int}	0.042	0.114	0.047
θ values (°)	θ_{max} = 29.6, θ_{min} = 3.5	θ_{max} = 25.0, θ_{min} = 3.3	θ_{max} = 33.0, θ_{min} = 1.9
$(\sin\theta/\lambda)_{max}$ (Å^{-1})	0.694	0.595	0.767
Range of *h*, *k*, *l*	$-17 \le h \le 16$, $-21 \le k \le 9$, $-43 \le l \le 28$	$-15 \le h \le 15$, $-16 \le k \le 17$, $-23 \le l \le 22$	$-16 \le h \le 8$, $-7 \le k \le 16$, $-15 \le l \le 9$
$R[F^2 > 2\sigma(F^2)]$, $wR(F^2)$, *S*	0.051, 0.125, 1.01	0.074, 0.182, 1.06	0.035, 0.110, 1.16
No. of reflections, parameters, restraints	4974, 343, 52	6230, 414, 78	507, 29, 0
H-atom treatment	H-atom parameters constrained	H-atom parameters constrained	H-atoms were nor refined
Weighting scheme	$w = 1/[\sigma^2(F_o^2) + (0.0706P)^2]$ where $P = (F_o^2 + 2F_c^2)/3$	$w = 1/[\sigma^2(F_o^2) + (0.0581P)^2 + 97.5865P]$ where $P = (F_o^2 + 2F_c^2)/3$	$w = 1/[\sigma^2(F_o^2) + (0.0523P)^2 + 20.1908P]$ where $P = (F_o^2 + 2F_c^2)/3$
$\Delta\rho_{max}$, $\Delta\rho_{min}$ (e Å^{-3})	3.51, -4.37	2.56, -2.35	2.42, -2.38

Experiments were carried out with Mo *K*α radiation.

Computer programs: *CrysAlis PRO* 1.171.38.41 (Rigaku OD, 2015), *APEX2* (Bruker-AXS, 2004), *SAINT* (Bruker-AXS, 2004), *SHELXS2014* (Sheldrick, 2014), *SHELXL2014* (Sheldrick, 2014), ShelXle (Hübschle, 2011), CIFTAB-2014 (Sheldrick, 2014).

Table S5. Selected geometric parameters (Å).

2			
O10—Co2	2.049 (18)	O6—W3	1.918 (14)
O11—Co2	2.111 (16)	O7—W2	1.931 (14)
O12—Co1	2.095 (17)	O7—W3	1.915 (15)
O19—Co1	2.054 (15)	O8—W1	1.981 (16)
O1—P1	1.52 (3)	O8—W2	1.889 (14)
O17—P1	1.556 (13)	O9—W1	1.672 (16)
O1—W4^{i}	2.464 (14)	O13—W2^{ii}	1.884 (14)
O1—W4^{ii}	2.464 (14)	O13—W2	1.926 (14)
O1—W4	2.464 (14)	O14—W2	1.714 (18)
O2—W4^{ii}	1.878 (14)	O15—W3	1.882 (16)
O2—W4	1.930 (15)	O15—W4	1.924 (16)
O3—W4	1.705 (19)	O16—W1	1.853 (17)
O4—W1^{ii}	1.898 (16)	O16—W4^{i}	1.945 (17)
O4—W3	1.916 (16)	O17—W1^{i}	2.426 (13)
O5—W3	1.730 (16)	O17—W2^{i}	2.417 (14)
O6—W1	1.914 (15)	O17—W3^{i}	2.445 (13)
3			
Ni1—N1	2.07 (2)	O11—W5	1.845 (19)
Ni1—N2	2.04 (2)	O12—W1	1.87 (2)
Ni1—N3	2.12 (2)	O12—W4	1.905 (18)
Ni1—N4	2.05 (2)	O13—W3	1.90 (2)
Ni1—N5	2.07 (2)	O13—W5	1.91 (2)
Ni1—N6	2.08 (3)	O14—W4	1.88 (2)
O18—P1	1.57 (3)	O14—W6^{iii}	1.93 (2)
O19—P1	1.59 (3)	O15—W2	1.86 (2)
O22—P1	1.49 (4)	O15—W6	1.94 (2)
O23—P1	1.43 (3)	O16—W1	1.90 (2)
O1—W5	1.699 (19)	O16—W6	1.90 (3)
O2—W4	1.86 (2)	O17—W1	1.94 (3)
O2—W5	1.89 (2)	O17—W2	1.85 (3)
O3—W4	1.70 (2)	O18—W1	2.43 (3)
O4—W3^{iii}	1.918 (18)	O18—W2	2.41 (3)
O4—W4	1.872 (19)	O18—W6	2.53 (3)
O5—W2	1.94 (2)	O19—W4	2.45 (3)
O5—W3	1.863 (19)	O19—W5	2.37 (3)
O6—W6	1.649 (17)	O19—W6^{iii}	2.51 (3)
O7—W1^{iii}	1.90 (2)	O20—W5^{iii}	1.93 (2)
O7—W3	1.90 (2)	O20—W6	1.85 (2)

O8—W1	1.689 (19)	O21—W3	1.71 (3)
O10—W2	1.665 (18)	O22—W3	2.38 (4)
O11—W2	1.935 (19)	O23—W3	2.50 (3)
4			
O3—Ge1	1.76 (2)	O2—W1	1.659 (11)
O1B—W1^{iv}	1.850 (4)	O3—W1^{iv}	2.342 (10)
O1B—W1	1.850 (4)	O3—W1^{v}	2.342 (10)
O1A—W1^{iv}	2.046 (7)	O3—W1	2.342 (10)
O1A—W1	2.046 (7)		

Symmetry code(s): (i) -*y*+1, *x*-*y*+1, *z*; (ii) -*x*+*y*, -*x*+1, *z*; (iii) -*x*+1, -*y*+2, -*z*+1; (iv) *y*, -*z*+1, *x*; (v) *z*, -*x*+1, -*y*+1.